

Nucleotide Recognition and Phosphate Linkage Hydrolysis at a Lipid Cubic Interface

Sergio Murgia,^{*,†} Sandrina Lampis,[†] Paolo Zucca,[‡] Enrico Sanjust,[‡] and Maura Monduzzi^{*,†}

Department of Chemical Science and Department of Biomedical Science and Technologies, Cagliari University, CNBS and CSGL, ss 554, bivio Sestu, 09042 Monserrato (CA), Italy

Received August 4, 2010; E-mail: murgias@unica.it; monduzzi@unica.it

Abstract: Mononucleotides, when entrapped within a mono-olein-based cubic *la3d* liquid crystalline phase, have been found to undergo hydrolysis at the sugar–phosphate ester bond in spite of their natural inertness toward hydrolysis. Here, kinetics of the hydrolysis reaction and interactions between the lipid matrix and the mononucleotide adenosine 5′-monophosphate disodium salt (AMP) and its 2′-deoxy derivative (dAMP) are thoroughly investigated in order to shed some light on the mechanism of the nucleotide recognition and phosphate ester hydrolysis. Experiments evidenced that molecular recognition occurs essentially through the *sn*-2 and the *sn*-3 alcoholic OH groups of mono-olein. As deduced from the apparent activation energies, the mechanism underlying the hydrolysis reaction is the same for AMP and dAMP. Nevertheless, the reaction proceeds slower for the latter, highlighting a substantial difference in the chemical behavior of the two nucleotides. A model that explains the hydrolysis reaction is presented. Remarkably, the hydrolysis mechanism appears to be highly specific for the *la3d* phase.

Introduction

Driven by hydrophobic/hydrophilic intermolecular interactions, several classes of polar lipids such as phospholipids or monoglycerides may self-assemble in water in a variety of nanostructured aggregates whose interfacial curvature and topology mainly depend on the constraints imposed by the lipid packing parameter, v/a_0l (v is the hydrophobic chain volume, a_0 is headgroup area, and l is the chain length, taken as the 80% of the fully extended chain).^{1,2}

Among these self-assembled nanostructures, the bicontinuous cubic phases possibly represent the most outstanding. These liquid-crystalline phases are constituted by curved, triply periodic non-intersecting bilayers organized to form two disjoint continuous water channels. Interestingly, the surface obtained by placing a plane in the gap between the end groups of the lipid bilayer of the cubic phase can be described by an infinite periodic minimal surface (IPMS). Three types of IPMSs, describing different cubic space groups, are important in lipid-based systems: the double diamond (primitive lattice, *Pn3m*), the gyroid (body-centered lattice, *Ia3d*), and the primitive type (body-centered lattice, *Im3m*).^{3,4} The two IPMSs relevant for this work are shown in Figure 1.

Because of their peculiar bilayer structure which closely resembles that of cell membranes, since their discovery in the

early 1980s, lipid bicontinuous cubic phases have attracted much attention, especially as biomimetics and drug delivery systems.⁵ Particularly significant also are their nanometric dispersions in water solution, known as cubosomes (the nonlamellar analogue of liposomes).⁶

It is worth noticing that these amazing IPMS assemblies are ubiquitous in all kingdoms, being found in conjunction with virtually all cell membranes.⁴ Indeed, thanks to electron microscopy studies, their textures were observed in living organisms well before their triply periodic arrangements were understood.⁷ Though found also under physiological conditions, cubic membranes are often associated with particular cellular stresses (e.g., starvation or drug treatments) or pathological states (e.g., infections or tumors).^{8,9} However, whether these membranes form as a result of anomalous membrane protein and/or lipid interactions in pathological states, or they are specific cellular response to these pathologies, is still a matter of debate. So far, the role of cubic membranes in the cell machinery has not fully been elucidated.

Recently, AMP, GMP, UMP, and CMP nucleotides (adenosine, guanosine, uridine, and cytidine 5′-monophosphate disodium salts, respectively) and two hydrophobically modified nucleotides were entrapped within a mono-olein (MO)-based *Ia3d*

[†] Department of Chemical Science.

[‡] Department of Biomedical Science and Technologies.

- (1) Israelachvili, J. N.; Mitchell, D. J.; Ninham, B. W. *J. Chem. Soc., Faraday Trans. 2* **1976**, *72*, 1525.
- (2) Mitchell, D. J.; Ninham, B. W. *J. Chem. Soc., Faraday Trans. 2* **1981**, *77*, 601.
- (3) Hyde, S. T. *J. Phys. Chem.* **1989**, *93*, 1458.
- (4) Hyde, S.; Andersson, S.; Larsson, K.; Blum, Z.; Landh, T.; Lidin, S.; Ninham, B. W. *The Language of Shape*; Elsevier: Amsterdam, 1997; Vol. 1, Chap. 5.

- (5) Shah, J.; Sadhale, Y.; Chilukuri, D. M. *Adv. Drug Delivery Rev.* **2001**, *47*, 229.
- (6) Murgia, S.; Falchi, A. M.; Mano, M.; Lampis, S.; Angius, R.; Carnerup, A. M.; Schmidt, J.; Diaz, G.; Giacca, M.; Talmon, Y.; Monduzzi, M. *J. Phys. Chem. B* **2010**, *114*, 3518.
- (7) Almshergji, Z. A.; Landh, T.; Kohlwein, S. D.; Deng, Y. *Int. Rev. Cell Mol. Biol.* **2009**, *274*, 275.
- (8) Almshergji, Z. A.; Kohlwein, S. D.; Deng, Y. *J. Cell Biol.* **2006**, *173*, 839.
- (9) Almshergji, Z.; Hyde, S.; Ramachandran, M.; Deng, Y. *J. R. Soc. Interface* **2008**, *5*, 1023.

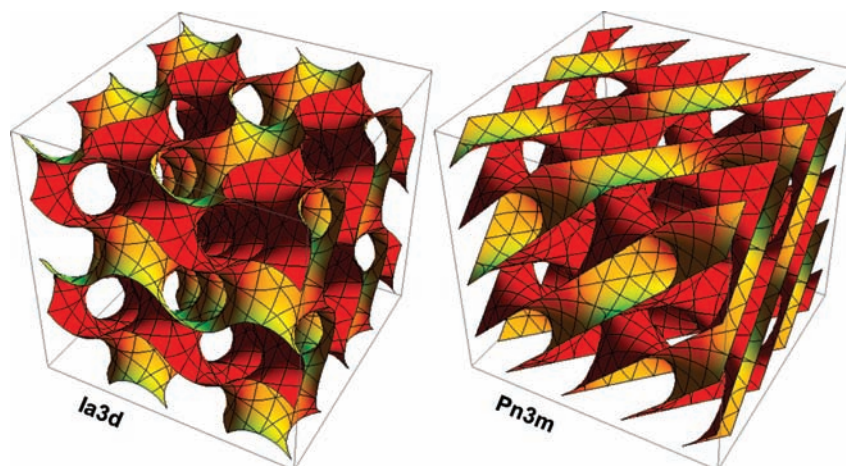


Figure 1. Gyroid (left) and double diamond (right) infinite periodic minimal surfaces.

cubic phase in order to assess the possible applications of such a lipid matrix in the drug delivery field.¹⁰ In that study, it was reported that nucleotides undergo a slow but significant phosphate ester hydrolysis, plainly induced by specific interactions at the mono-olein–water interface. Bearing in mind the natural inertness toward hydrolysis displayed by phosphate monoester dianions in the absence of catalytic agents, such a result was really surprising. In addition, upon aging, a cubic to hexagonal phase transition of the samples was detected at room temperature, while in the MO/water binary system hexagonal liquid crystals form only above 70 °C.

Here, AMP and its 2'-deoxy derivative (dAMP), entrapped inside the MO-based cubic *Ia3d* liquid crystalline phase, were investigated to determine at which site of the lipid interface the nucleotide recognition occurs and to achieve a deeper understanding of the mechanism that drives the phosphate ester hydrolysis.

The hydrolysis of phosphate monoesters is of fundamental importance in biological systems, being involved in processes that range from signaling to energy transduction. Consequently, this topic has been extensively studied in the past by theoretical and experimental approaches.^{11,12} Nevertheless, the mechanism through which hydrolysis proceeds is a controversial matter. Indeed, phosphate monoester hydrolysis could in principle proceed through two main alternative mechanisms (see below for intermediate mechanisms): (i) an *associative* bimolecular mechanism where the nucleophilic attack to the phosphorus atom involves a temporary increase of its coordination from four to five and a subsequent alcohol (or phenol) expulsion to restore the tetrahedral geometry of the arising orthophosphate or (ii) a *dissociative* mechanism where the coordination number of phosphorus temporarily decreases from four to three, somewhat paralleling the acylium ion mechanism for carboxylic ester hydrolysis.¹³ The controversy between the supporters of the two alternative mechanisms has produced, over several decades, a huge number of both experimental data and theoretical calculations, and therefore many articles keep the debate

quite topical.^{14,15} In fact, several experimental studies have shown the existence of the very elusive metaphosphate as the intermediate in monoester hydrolysis.^{16–18} More recently, it was established that the dissociative mechanism involving metaphosphate is energetically favored compared to the associative one.¹⁹ This is particularly true in the case of monoalkyl phosphates in their monoanionic state, where a proton transfer to the ester bridging oxygen is a prerequisite for the subsequent metaphosphate anion dissociation and alcohol release.²⁰ In other words, such a proton transfer allows for the release of alcohol instead of the relatively disfavored alkoxide ion. It is worth underlining that this proton transfer could take place even more easily when a water molecule participates in the formation of a six-membered cyclic transition state.¹⁹ At least in the case of monoalkylphosphates, the so-called substrate-assisted catalysis has been judged as unlikely.^{21,22}

Nevertheless, some evidence supports the importance of loose concerted mechanisms.²³ In fact, by placing the leaving RO group at an axial position of the phosphorane-like intermediate (or rather transition state, when a prevailing dissociative character of the mechanism is hypothesized), the latent planar trigonal structure of the metaphosphate anion becomes evident.

Apart from its speculative interest, the whole controversy is of the highest importance when attempting to explain the mechanism of phosphoryl-transfer reactions (with the outstanding case of transfer to water, i.e., phosphate ester hydrolysis) catalyzed by the various classes of phosphatases.

In the case of phosphate monoesters, a crucial consideration deals with the actual protonation state of the species to be

(10) Murgia, S.; Lampis, S.; Angius, R.; Berti, D.; Monduzzi, M. *J. Phys. Chem. B* **2009**, *113*, 9205.
 (11) Klähn, M.; Rosta, E.; Warshel, A. *J. Am. Chem. Soc.* **2006**, *128*, 15310.
 (12) López-Canut, V.; Martí, S.; Bertrán, J.; Moliner, V.; Tuñón, I. *J. Phys. Chem. B* **2009**, *113*, 7816.
 (13) Westheimer, F. H. *Chem. Rev.* **1981**, *81*, 313.

(14) Åqvist, J.; Kolmodin, K.; Florian, J.; Warshel, A. *Chem. Biol.* **1999**, *6*, R71.
 (15) Baxter, N. J.; Bowler, M. W.; Alizadeh, T.; Cliff, M. J.; Hounslow, A. M.; Wu, B.; Berkowitz, D. B.; Williams, N. H.; Blackburn, G. M.; Waltho, J. P. *Proc. Natl. Acad. Sci. U.S.A.* **2010**, *107*, 4555.
 (16) Scott, L. T.; Rebek, J.; Ovsyanko, L.; Sims, C. *J. Am. Chem. Soc.* **1977**, *99*, 625.
 (17) Henschman, M.; Viggiano, A. A.; Paulson, J. F.; Freedman, A.; Wormhoudt, J. *J. Am. Chem. Soc.* **1985**, *107*, 1453.
 (18) Friedman, J. M.; Freeman, S.; Knowles, J. R. *J. Am. Chem. Soc.* **1988**, *110*, 1268.
 (19) Hu, C. H.; Brinck, T. *J. Phys. Chem. A* **1999**, *103*, 5379.
 (20) Bianciotto, M.; Barthelat, J.-C.; Vigroux, A. *J. Am. Chem. Soc.* **2002**, *124*, 7573.
 (21) Admiraal, S. J.; Herschlag, D. *J. Am. Chem. Soc.* **2000**, *122*, 2145.
 (22) Iché-Tarrat, N.; Ruiz-Lopez, M.; Barthelat, J.-C.; Vigroux, A. *Chem. Eur. J.* **2007**, *13*, 3617.
 (23) Cleland, W. W.; Hengge, A. C. *Chem. Rev.* **2006**, *106*, 3252.

hydrolyzed. Indeed, the dianions (the form prevailing at neutral and especially at alkaline pHs) are generally characterized by their exceptional kinetic inertness (a compulsory requisite in view of their biological roles), so that their mean half-life in the absence of chemical or enzymic catalysts is of about 1.1×10^{12} years!²⁴

Materials and Methods

Materials. Mono-olein (MO, 1-mono-oleoylglycerol, RYLO MG 90-glycerol mono-oleate; 98 wt % monoglyceride, also containing 8 wt % of 2-mono-oleoylglycerol and 5 wt % of mono-linoleoylglycerol as ascertained through a quantitative ¹³C NMR analysis) was kindly provided by Danisco Ingredients (Brabrand, Denmark). The nucleotide adenosine 5'-monophosphate, disodium salt AMP ($\geq 99.0\%$) is from Sigma, whereas 2'-deoxyadenosine 5'-monophosphate, disodium salt (dAMP) is from MP Biomedicals. Samples were prepared in deuterated water (D₂O, purchased from Cambridge Laboratory, Inc. with a purity of 99.9%) rather than distilled water for the sake of comparison with sample investigated in ref 10. Moreover, the use of D₂O avoided superimposition of H₂O hydroxyl signals with MO hydroxyl signals in the FT-IR spectra.

Sample Preparation. Samples were prepared by weighing the components into glass tubes that were homogenized by repeated cycles of centrifugation back and forth at 3000 rpm at 25 °C.

NMR Experiments. ¹H, ¹³C, and ³¹P NMR measurements were carried out at 25 °C using a Bruker Avance 300 MHz (7.05 T) spectrometer at the operating frequencies of 300.131, 75.475, and 121.495 MHz, respectively. A standard BVT 3000 variable-temperature control unit with an accuracy of ± 0.5 °C was used.

Quantitative evaluation of peak areas and determination of ³¹P NMR spin-lattice relaxation times (T_1) were performed by using a 10 mm wide-bore multinuclear probe. T_1 was measured by the standard inversion recovery sequence (180- τ -90) by acquiring the partially relaxed spectra at 14 different τ values. Experiments gave $T_1 = 2.43 \pm 0.08$ and 1.50 ± 0.09 s for the AMP and dAMP molecular species, respectively, in freshly prepared samples.

As to the quantitative analysis, conditions adopted were chosen in order to satisfy the rule which dictates that the sum of the acquisition time ($at = 1$ s) and the delay between two consecutive pulses ($D1 = 15$ s) must be greater than $5T_1$ ($at + D1 > 5T_1$) to allow a complete relaxation of the magnetization. (Repeated experiments using up to $D1 = 60$ s did not result in significant variation of the measured peak areas.) ¹H-decoupled ³¹P NMR spectra were acquired by exploiting an inverse gated pulse sequence to suppress the nuclear Overhauser effect (NOE) and by using a 90° pulse (12.5 μ s). Usually, 256 scans were performed to achieve an optimal signal-to-noise ratio. The quantitative analysis was carried out through an iterative fitting of the spectra (assuming a Lorentzian shape for the ³¹P NMR signals) to get the peak areas by the use of the program Microcal Origin (version 5.0) from Microcal Software, Inc. (Northampton, MA).

Self-diffusion coefficients were determined using a Bruker DIFF30 probe equipped with specific inserts for the ¹H and ³¹P nuclei and supplied by a Bruker Great 1/40 amplifier that can generate field gradients up to 1.2 T m⁻¹. The pulse-gradient stimulated echo (PGSTE) sequence was used. Self-diffusion coefficients were obtained by varying the gradient strength (g) while keeping the gradient pulse length (δ) and the gradient pulse intervals constant within each experimental run. The data were fitted according to the Stejskal-Tanner equation:

$$\frac{I}{I_0} = \exp\left[-Dq^2\left(\Delta - \frac{\delta}{3}\right)\right] \quad (1)$$

where I and I_0 are the signal intensities in the presence and absence of the applied field gradient, respectively, $q = \gamma g \delta$ is the so-called

scattering vector (γ being the gyromagnetic ratio of the observed nucleus), $t = (\Delta - \delta/3)$ is the diffusion time, Δ is the delay time between the encoding and decoding gradients, and D is the self-diffusion coefficient to be extracted.²⁵ Errors on the self-diffusion coefficient measurements are reported as standard deviation.

FT-IR Experiments. FT-IR spectra were recorded with a Bruker Tensor 27 spectrophotometer equipped with a BIO-ATR II module and N₂(_l)-cooled MCT detector. For each measurement, 64 scans were collected and Fourier transformed to obtain a nominal spectral resolution of 2 cm⁻¹ over the frequency range 900–4000 cm⁻¹. The BIO-ATR chamber was heat-controlled at 25 ± 0.1 °C. Samples were placed in the BIO-ATR, and a 10 min waiting time was used to allow the temperature to reach equilibrium before recording spectra. Before each measurement, the ATR crystal was cleaned with 2-propanol and distilled water and dried with a soft tissue until the baseline recorded ensured that no residue of the previous sample was retained. OPUS software (Bruker, Milan, Italy) was used for spectra analysis.

SAXS Experiments. The small-angle X-ray scattering (SAXS) was recorded with a S3-MICRO SWAXS camera system (HECUS X-ray Systems, Graz, Austria). Cu K α radiation of wavelength 1.542 Å was provided by a GeniX X-ray generator, operating at 50 kV and 1 mA. A 1D-PSD-50 M system (HECUS X-ray Systems) containing 1024 channels of width 54.0 μ m was used for detection of scattered X-rays in the small-angle region. The working q -range (Å^{-1}) was $0.003 \leq q \leq 0.6$, where $q = 4\pi \sin(\theta)\lambda^{-1}$ is the modulus of the scattering wave vector. A few milligrams of the sample was enclosed in a stainless steel sample holder using a polymeric sheet (Bratfolie, Kalle) window. The distance between the sample and detector was 235 mm. The diffraction patterns were recorded at 25 °C for 3600 s. To minimize scattering from air, the camera volume was kept under vacuum during the measurements. Silver behenate (CH₃-(CH₂)₂₀-COOAg) with a d spacing value of 58.38 Å was used as a standard to calibrate the angular scale of the measured intensity.

The lattice parameters (a) of the cubic phases were determined using the relation

$$d_{hkl} = \frac{2\pi}{q} = \frac{a}{(h^2 + k^2 + l^2)^{1/2}} \quad (2)$$

from linear fits of the plots of d_{hkl} versus $(h^2 + k^2 + l^2)^{-1/2}$. Here, d_{hkl} is the spacing of Bragg reflections, q is the measured peak position, and h , k , and l are the Miller indices. For the correct choice of space group, this plot gives a straight line passing through the origin and having a slope of the lattice parameter a .

Water channels radii, R_w , were calculated according to^{4,26,27}

$$R_w = \left(\frac{A_0}{-2\pi\chi}\right)^{1/2} a - L \quad (3)$$

where L is the lipid length value (17 Å),⁴ a is the lattice parameter obtained from the SAXS analysis, and A_0 and χ are the surface area and the Euler characteristic of the IPMS geometries ($Ia3d$, $A_0 = 3.091$, $\chi = -8$; $Pn3m$, $A_0 = 1.919$, $\chi = -2$).

Results and Discussion

As previously reported on a qualitative base, inclusion of AMP within a MO-based $Ia3d$ cubic phase results in the slow hydrolysis of the ribose-phosphate ester bond caused by specific interactions at the MO-water interface. The occurrence of the hydrolysis reaction was revealed by the growth of a new resonance in the ³¹P NMR spectrum upon the samples aging,

(25) Stejskal, E. O.; Tanner, J. E. *J. Chem. Phys.* **1965**, *42*, 288.

(26) Andersson, S.; Hyde, S. T.; Larsson, K.; Lidin, S. *Chem. Rev.* **1988**, *88*, 221.

(27) Briggs, J.; Chung, H.; Caffrey, M. *J. Phys. II Fr.* **1996**, *6*, 723.

(24) Lad, C.; Williams, N. H.; Wolfenden, R. *Proc. Natl. Acad. Sci. U.S.A.* **2003**, *100*, 5607.

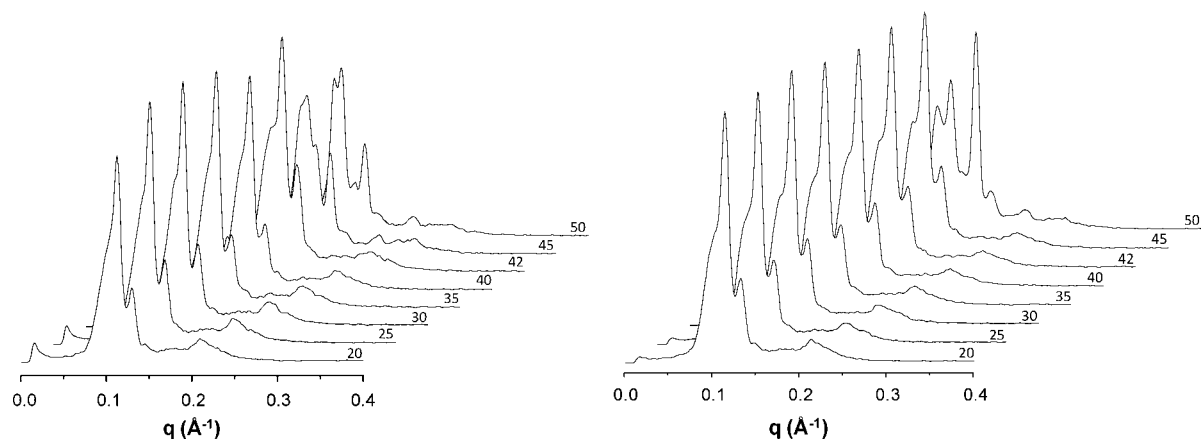


Figure 2. Stack plot of SAXS diffractograms recorded at different temperatures (reported in °C) of the MO/D₂O = 70/30 *Ia3d* cubic phase containing either AMP (a, left) or dAMP (b, right).

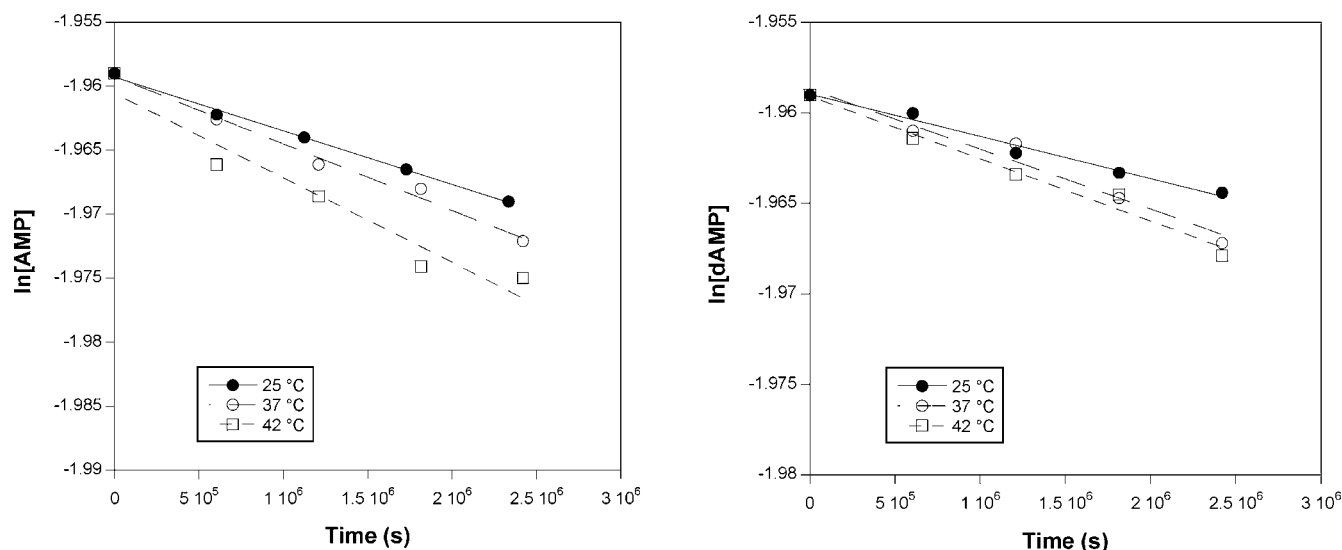


Figure 3. Kinetic plots obtained at various temperatures for the hydrolysis of 1.5 wt % AMP (left) or dAMP (right) nucleotides entrapped within the MO/D₂O = 70/30 *Ia3d* cubic phase.

while the reaction product (HPO_4^{2-}) was basically assessed through the determination of its chemical shift and self-diffusion coefficient.

The present investigation started with some preliminary NMR experiments conducted on a MO/D₂O = 70/30 *Ia3d* sample containing 1.5 wt % of dAMP to ascertain possible differences at either the macroscopic or the molecular level with respect to the AMP-containing system. As a matter of fact, no differences were noted in the ³¹P NMR chemical shifts nor in the self-diffusion coefficient values of the nucleotide, as determined through ³¹P NMR PGSTE experiments ($D_{\text{dAMP}} = (3.1 \pm 0.1) \times 10^{-11} \text{ m}^2/\text{s}$, to be compared with the value $D_{\text{AMP}} = (3.2 \pm 0.2) \times 10^{-11} \text{ m}^2/\text{s}$ reported in ref 10). More significantly, in much the same way as AMP, dAMP molecules when entrapped within the water channels of the liquid crystalline matrix undergo the hydrolysis process upon sample aging. These results essentially confirm, on a qualitative basis, that dAMP behaves similarly to AMP.

To shed some light on the reaction mechanism, the hydrolysis of the two nucleotides entrapped in the MO/D₂O *Ia3d* cubic phase was quantitatively followed by recording the ³¹P NMR spectra of the samples at 25 °C over a period of 1 month. In

addition, considering the possible biological implications of this study, experiments were repeated at 37 and 42 °C.

Since variations in temperature may induce phase transitions, the temperature dependence of the MO/D₂O = 70/30 samples containing either AMP or dAMP was investigated through SAXS. Results related to AMP are depicted in Figure 2a. The system under study is a pure *Ia3d* phase up to at least 42 °C, whereas an *Ia3d* to *Pn3m* inter-cubic phase transition takes place starting from 45 °C. A slightly different phase behavior is detected for dAMP, as reported in Figure 2b. Actually, in the latter case the phase transition begins at 50 °C. It is here worth noticing that, in the MO/D₂O = 70/30 binary system, this kind of phase transition was not observed up to 55 °C (data not shown). Therefore, from these experiments it can be concluded that interactions of nucleotides with the lipid matrix favor the *Ia3d* to *Pn3m* phase transition, and this effect is stronger for AMP than for dAMP.

Results concerning the ³¹P NMR quantitative analysis are shown in Figure 3. As can be clearly noted, the exponential consumption of AMP and dAMP during the time course confirmed that the hydrolysis reaction occurs as a first-order process with respect to the substrate, meaning that MO acts

Table 1. Apparent Kinetic Rate Constants, k ($\times 10^9 \text{ s}^{-1}$), of the Nucleotide Hydrolysis Reaction Estimated at Different Temperatures, Indicated in $^{\circ}\text{C}$ as Subscripts (Also Reported Are the Standard Errors Determined by Regression)

nucleotide	k_{25}	k_{37}	k_{42}
AMP	4.2 ± 0.2	5.2 ± 0.3	6.6 ± 0.9
dAMP	2.3 ± 0.2	3.3 ± 0.3	3.4 ± 0.3

like a catalyst rather than a reactant. This finding is in agreement with the self-diffusion coefficient value of the hydrolyzed phosphate moiety,¹⁰ which rules out the possibility that the new phosphorus-bearing species is covalently bound to the MO molecules. Accordingly, no changes were observed in the MO ^{13}C NMR spectra recorded immediately after sample preparations and several months after the conclusion of the experiments.

The apparent kinetic rate constants, k , for both nucleotides were determined by taking the slope of a fitted linear regression curve. Results are reported in Table 1.

As commonly observed, the rate of the hydrolysis increases as the temperature increases. Nevertheless, and quite remarkably, compared to AMP, the dAMP k values are almost halved. Repeated experiments gave a percentage error on the estimated k values around 10%; therefore, the striking difference found for the apparent kinetic rate constants of the two nucleotides should be considered as highly significant. This implies that the simple absence of the hydroxyl group in the 2'-position of the dAMP molecule strongly affects the hydrolysis process rate.

The temperature dependence of a kinetic rate constant is typically described in terms of the Arrhenius equation: $k = A e^{-E_a/RT}$. The activation energy E_a was evaluated from the Arrhenius plot shown in Figure 4. The calculated E_a values were 18.9 and 18.0 kJ/mol for the AMP and the dAMP molecules, respectively. Although activation energies for the phosphoester bond hydrolysis previously reported in both experimental and theoretical works covered a quite broad range, from 9.5 (for a very efficient inositol monophosphatase)²⁸ to about 180 kJ/mol,^{11,29} values here obtained appear to be rather low. Indeed, it is hard to believe that the system under investigation may lower the activation barrier of the hydrolysis reaction with an efficiency close to that of enzymes, even considering the important role that the discrete water structures found in MO-

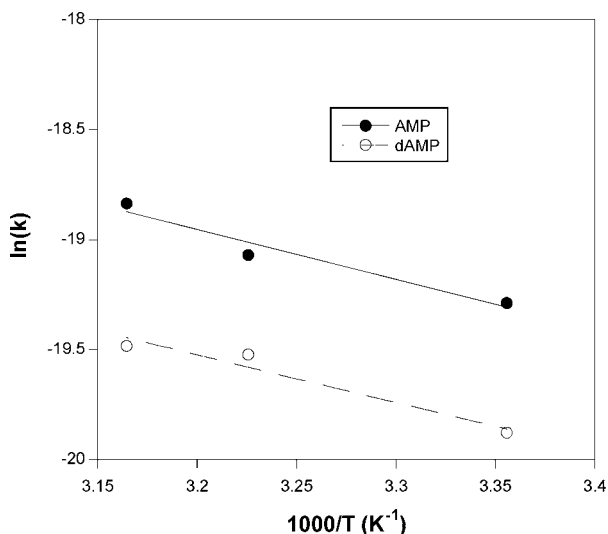


Figure 4. Arrhenius plot of the apparent kinetic rate constants of either 1.5 wt % AMP or dAMP nucleotides entrapped within the MO/D₂O = 70/30 *Ia3d* cubic phase.

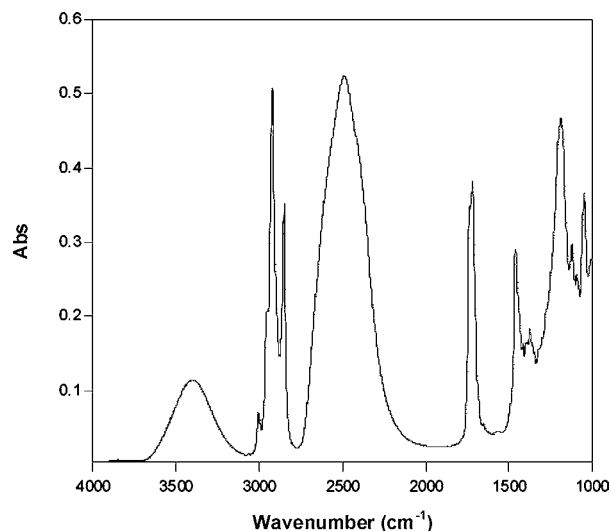


Figure 5. FT-IR spectrum of the *Ia3d* cubic phase with composition MO/D₂O = 70/30 at $T = 25$ $^{\circ}\text{C}$.

based cubic phases³⁰ may express in stabilizing the transition state. Nevertheless, bearing in mind the peculiar morphological characteristics of the cubic phase (which closely resembles that of porous catalysts like zeolites) where the hydrolysis reaction takes place, the observed E_a values seem less surprising. In fact, these low E_a values can be considered as the signature of a diffusion-controlled process, a regime where the measured E_a is expected to be lower than that in the absence of diffusion processes which constitute the rate-determining step.³¹ Consequently, E_a values (and k as well) reported here should be taken as *apparent* rather than absolute.

Though based on three temperatures only, results indicate that the same apparent activation energy pertains to the hydrolysis reaction of both nucleotides and, consequently, strongly suggest that the mechanism underlying the process is the same. Hence, a different probability (enclosed in the pre-exponential factor A) in the formation of the reaction intermediates can be called into play to justify the observed apparent kinetic rate constants. Moreover, the MO-water interface undoubtedly plays a crucial role in the reaction mechanism; thus, every reasonable hypothesis aimed at clarifying the retardation in the dAMP hydrolysis should consider the slightly different hydrophilicity of the two nucleotides and its implication on the molecular adhesion and displacement at the lipid interface. This deduction can be corroborated by the FT-IR analysis of the samples.

The FT-IR spectrum of the *Ia3d* cubic phase with composition MO/D₂O = 70/30 is shown in Figure 5. FT-IR spectra of lipid aggregates are conveniently analyzed by separately observing the hydrophobic acyl chain and the hydrophilic headgroup regions. The stretching mode of CH=CH can be found at 3004 cm^{-1} and the symmetric stretching mode of the methylene group at 2853 cm^{-1} .^{32,33} The methylene wagging modes of n -alkanes

(28) Nigou, J.; Dover, L. G.; Besra, G. S. *Biochemistry* **2002**, *41*, 4392.

(29) Bel'skii, V. E. *Russ. Chem. Rev.* **1977**, *46*, 828.

(30) Jongjoo, K.; Wenyun, L.; Weihong, Q.; Lijuan, W.; Caffrey, M.; Dongping, Z. *J. Phys. Chem. B* **2006**, *110*, 21994.

(31) Thomas, J. M.; Thomas, W. J. *Heterogeneous Catalysis*; VCH: Weinheim, 1997.

(32) Mantsch, H. H.; Martin, A.; Cameron, D. G. *Biochemistry* **1981**, *20*, 3138.

(33) Nilsson, A.; Holmgren, A.; Lindblom, G. *Chem. Phys. Lipids* **1994**, *69*, 219.

Table 2. Peak Frequencies and Bandwidths of Lipid Alcoholic *sn*-2 and *sn*-3 C–OH Bands in MO/D₂O = 70/30 Cubic Samples Also Containing 1.5 wt % of Nucleotide

sample	peak frequency ^a (cm ⁻¹)	bandwidth ^a (cm ⁻¹)	band
MO/D ₂ O	1121.2	17.1	<i>sn</i> -2 C–OH
MO/D ₂ O/AMP 1.5 wt %	1120.3	18.5	
MO/D ₂ O/dAMP 1.5 wt %	1120.2	17.9	
MO/D ₂ O	1050.8	25.7	<i>sn</i> -3 C–OH
MO/D ₂ O/AMP 1.5 wt %	1051.0	24.4	
MO/D ₂ O/dAMP 1.5 wt %	1051.1	24.3	

^a Uncertainty is lower than ± 0.1 cm⁻¹.

are observed in the range 1330–1390 cm⁻¹.^{34–37} The bands of interest represent the gauche-*trans*-gauche (kink, 1368 cm⁻¹), double gauche (gg, 1353 cm⁻¹), and end gauche (eg, 1341 cm⁻¹) conformations. The bending of terminal –CH₃ (umbrella mode) is found at 1378 cm⁻¹ and can be used for normalization of other intensities, being insensitive to the lipids' conformation state.³³ Previous studies³⁶ suggested that insertion of polar probes into the liquid-crystalline cubic phases could affect the acyl chain order, modifying the proportion of these conformers. However, no significant difference was detected in nucleotides-containing samples, suggesting their possible action to be limited to the polar region. In this region, four major MO vibrational modes can be observed, related to the stretching of the bonds *sn*-1 CO–O (ester, ~ 1180 cm⁻¹), *sn*-1 C=O (carbonyl, ~ 1720 and 1740 cm⁻¹, respectively H-bonded and free C=O), *sn*-2 C–OH (~ 1120 cm⁻¹), and *sn*-3 C–OH (~ 1050 cm⁻¹).^{33,35,36,38,39} With regard to the first band, its frequency shifts were proposed as a result of a slight deviation from the dihedral angle of 180° in C₃–C₂–C₁O–O–C segment.^{36,37,40} Also in this case, no significant changes were observed because of inclusion of mononucleotides within the liquid-crystalline cubic phases. Analogous results were also recorded for *sn*-1 C=O bands, in good agreement with previously reported studies on protein inclusion on similar lipid phases.³⁶ In that work, a low-frequency shift of the *sn*-3 C–OH band was correlated with more polar surroundings of the bond. In the samples under investigation, as reported in Table 2, a similar significant shift was observed only for the *sn*-2 C–OH band, apparently suggesting a similar effect.

More remarkable information on the nucleotide interactions with the MO polar head was obtained from the changes induced on the *sn*-2 and *sn*-3 C–OH bandwidths.

While it was previously noted that cytochrome *c* inclusion in MO cubic phases broadened both bands,³⁶ here a diverse effect on *sn*-2 and *sn*-3 C–OH bands was observed. Indeed, the former was broadened by the presence of both AMP and dAMP, but to different extents. Conversely, a noteworthy narrowing of the latter was detected in both nucleotide-containing samples. These experimental findings can be associ-

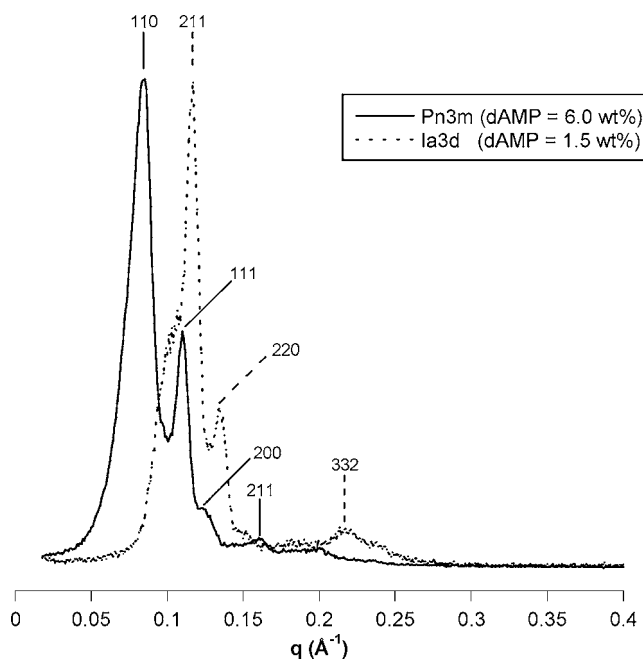


Figure 6. SAXS diffractograms at $T = 25$ °C of samples with composition MO/D₂O = 70/30 containing 1.5 wt % (dotted line) and 6.0 wt % (continuous line) of dAMP. The Miller indices *hkl* are given for each reflection.

ated with a close interaction between MO polar heads and nucleotides. The absence of the 2'-hydroxyl group somewhat modifies the degree of this interaction.

On the whole, FT-IR data indicate that inclusion of 1.5 wt % of nucleotide does not affect the organization of the cubic-phase hydrophobic portion. On the contrary, nucleotides/MO interactions take place at the lipid polar head region, with the specific involvement of the *sn*-2 and the *sn*-3 alcoholic OH groups. Particularly, the measured variations in the bandwidths of these groups suggest that the nucleotides/interface interactions are stronger for AMP than dAMP. However, since only small differences were observed between AMP- and dAMP-containing cubic phases, it can be concluded that very similar interactions occur in both samples.

In order to further clarify the subtle interactions occurring between the nucleotides and the MO interface, two samples with composition MO/D₂O = 70/30 and containing 6.0 wt % of either AMP or dAMP were also prepared. As revealed by SAXS analysis (see Figure 6), the inclusion of such an amount of nucleotides within the cubic samples is sufficient to induce the occurrence of a *Pn3m* cubic phase, even in freshly prepared samples. It deserves note that this kind of intercalation transition is identical to that provoked by the addition of 0.8 wt % of Na₂HPO₄ to the MO/D₂O = 70/30 cubic phase.¹⁰

FT-IR measurements performed on samples containing 6.0 wt % of nucleotides were affected by a high uncertainty due to the growing phosphate peak in the proximity of the *sn*-2 and *sn*-3 OH peaks.

Turning the attention to the SAXS data, the structural investigation of the *Pn3m* phase gives, from the linear fit of the d_{hkl} vs $(h^2 + k^2 + l^2)^{-1/2}$ plot reported in Figure 7, the lattice parameters $a = 84.5 \pm 0.4$ and 89.1 ± 0.6 Å (correlation coefficients $r_{AMP} = 0.9998$ and $r_{dAMP} = 0.9994$) and water channel radius $R_W = 16.0$ and 17.9 Å for the AMP- and dAMP-containing systems, respectively. Recalling here that the hydrophobic portion of the cubic phase remains unaltered by

(34) Senak, L.; Davies, M. A.; Mendelsohn, R. *J. Phys. Chem.* **1991**, *95*, 2565.

(35) Nilsson, A.; Holmgren, A.; Lindblom, G. *Chem. Phys. Lipids* **1994**, *71*, 119.

(36) Razumas, V.; Larsson, K.; Mieziš, Y.; Nylander, T. *J. Phys. Chem.* **1996**, *100*, 11766.

(37) Razumas, V.; Talaikytė, Z.; Barauskas, J.; Mieziš, Y.; Nylander, T. *Vibr. Spectrosc.* **1997**, *15*, 91.

(38) Holmgren, A.; Lindblom, G.; Johansson, L. B. A. *J. Phys. Chem.* **1988**, *92*, 5639.

(39) Lendermann, J.; Winter, R. *Phys. Chem. Chem. Phys.* **2003**, *5*, 1440.

(40) Hübner, W.; Mantsch, H. H. *Biophys. J.* **1991**, *59*, 1261.

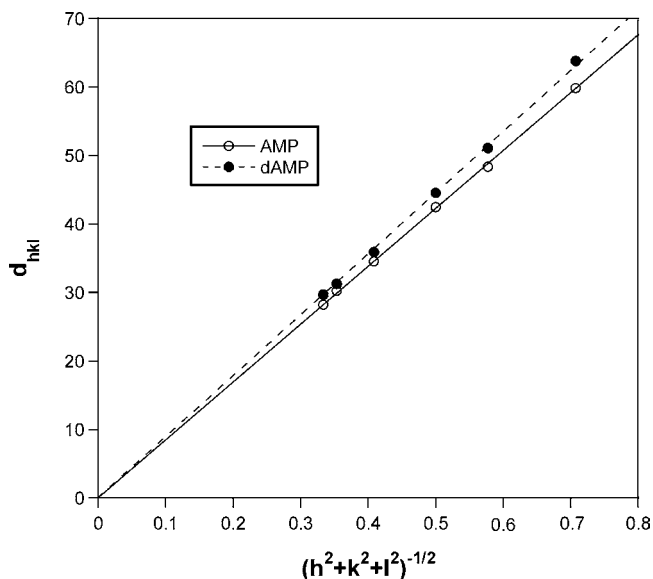


Figure 7. Plot of d_{hkl} (Å) vs $(h^2 + k^2 + l^2)^{-1/2}$ of the reflections observed in the SAXS analysis of the *Pn3m* samples obtained loading the MO/D₂O = 70/30 system with either 6.0 wt % AMP or dAMP.

inclusion of the nucleotides (from the FT-IR analysis), and since the v/a_0l ratio is bigger for the *Pn3m* than for the *Ia3d* cubic phase,⁴¹ the observed phase behavior necessarily requires a decrease of the effective polar head area. This fact is in accordance with the proposed mechanism for the phase transition, which entails a phosphate bridging between two MO molecules that favors the reduction of the polar head area. Nevertheless, the small differences in a and R_w values, assessed through the SAXS analysis, strongly suggest different specific interactions of the two nucleotides, as dictated by the presence/absence of the hydroxyl group in the 2'-position. Indeed, these results implicitly support the existence of stronger interactions between the MO interface and AMP with respect to dAMP since a decrease of the (reverse) interface curvature (smaller R_w) can be assumed as a straightforward consequence of a greater v/a_0l ratio. This result perfectly matches the previously discussed nucleotides-induced effects on the temperature dependence of the phase transition (cf. Figure 2) and hydrolysis rate (cf. Table 1 and Figure 3) observed in the two MO/W/(d)AMP systems.

³¹P NMR PGSTE experiments on cubic samples loaded with 6.0 wt % of either AMP or dAMP yield self-diffusion coefficients of $(1.20 \pm 0.06) \times 10^{-11}$ m²/s for both nucleotides. Compared with the self-diffusion coefficient of $(3.2 \pm 0.2) \times 10^{-11}$ m²/s measured for the AMP molecules in an *Ia3d* cubic phase containing 1.5 wt % of nucleotide, this value indicates that nucleotides diffusion is reduced to about one-third. This experimental finding deserves some consideration.

The concept that underpins the study of the molecular motions is based on the simple observation that the self-diffusion coefficient of a molecule is altered by a specific interaction with another molecule or by a restriction of the molecular displacement. In the present investigation, molecular motions within the bicontinuous cubic environment are subjected to the monodimensional constraint imposed by the peculiar topology of these systems. Therefore, with respect to molecules that can freely move along all possible directions (e.g., in a water

solution), since they are forced to move within the water channels, a two-thirds reduction of the self-diffusion coefficient is predictable (and usually observed) for molecules residing within *Ia3d* or *Pn3m* cubic phases. Moreover, if specific interactions causing molecules to bind to the interface occur, a further decrease of the observed D value (D^{obs}) is expected according to the well-known Lindman equation:

$$D^{\text{obs}} = pD^{\text{bound}} + (1-p)D^{\text{free}} \quad (4)$$

where p is the molar fraction of the molecules bound to the interface while D^{bound} and D^{free} represent the molecules' self-diffusion coefficients in the bound and free states.

Slightly overestimated p values may be calculated from eq 4, assuming that the nucleotide D^{bound} equals the MO self-diffusion coefficients. These were assessed through ¹H PGSTE measurements and found equal to $(1.12 \pm 0.04) \times 10^{-11}$ and $(0.90 \pm 0.03) \times 10^{-11}$ m²/s in the *Ia3d* and *Pn3m* cubic phases, respectively, containing 1.5 and 6.0 wt % of nucleotide. Therefore, taking one-third of the D value measured for the nucleotides in a 0.2 M water solution $((2.68 \pm 0.06) \times 10^{-10}$ m²/s) as D^{free} , p values of 0.73 and 0.96 were calculated for the *Ia3d* (1.5 wt % of nucleotide) and *Pn3m* (6.0 wt % of nucleotide) cubic phases, respectively. Within the uncertainties posed by the assumptions made, these values undoubtedly show the high affinity of the nucleotides for the lipid interface and, at the same time, evidence the shift toward the bound state of the nucleotide upon increasing its concentration.

A 4-fold increase of the nucleotide concentration along with a stronger binding to the MO interface would have resulted in an increase of the hydrolysis rate. Surprisingly, the opposite effect was observed. Indeed, even after 2 months, no hydrolysis was detected in both AMP- and dAMP-loaded MO/W samples. Nevertheless, as noted for the case of the cubic phases containing 1.5 wt % of nucleotide, samples remain isotropic for at least 1 month, and then traces of birefringence start to appear at visual inspection through crossed polaroids. These apparently counterintuitive results can be properly contextualized as follows.

The *Ia3d* to *Pn3m* inter-cubic transition was previously observed in freshly prepared samples upon 0.8 wt % addition of Na₂HPO₄.¹⁰ Here, the same effect can be observed upon 6.0 wt % addition of (d)AMP. These findings lead to the logical conclusion that both nucleotides and their hydrolysis products can be called into play for the phase transition, but the hydrogen phosphate anion accelerates this process. On the other hand, to explain the absence of hydrolysis detected in *Pn3m* samples, it is necessary to admit that the different local constraints imposed at the lipid molecules in the double diamond liquid-crystalline phase (cfr. Figure 1) do not allow the mechanism at the basis of the hydrolysis reaction to be explicated.

Mechanism of the Hydrolysis Reaction. Both AMP and dAMP uncatalyzed hydrolysis was found to be extraordinarily slow, regardless of the presence or absence of 2'-OH. However, their phosphoester bond can easily be hydrolyzed by some enzymes known as 5'-nucleotidases that have been studied in detail.⁴² Chemical, base-catalyzed hydrolysis of the 5'-phosphoester linkage is a well-known phenomenon for di- and polyribonucleotides such as RNA, where the 2'-OH gives an anchimeric assistance for the hydrolysis of the 5'-ester linkage with the *adjacent* ribose. The reaction goes through a 2',3'-cyclic phosphoester, and the reaction product is a mixture of

(41) Razumas, V.; Niaura, G.; Talaikytyė, Z.; Vagonis, A.; Nylander, T. *Biophys. Chem.* **2001**, *90*, 75.

(42) Zimmermann, H. *Biochem. J.* **1992**, *285*, 345.

3'- and 2'-monoesters. Also the enzyme ribonuclease uses a quite similar mechanism where the base is a histidine residue in the active site, but the 3'-monoester is the sole reaction product. Clearly, the deoxyribonuclease uses a completely different mechanism, as DNA lacks any 2'-OH that the enzyme could exploit. In contrast to RNA, DNA is resistant against base-catalyzed hydrolysis of its phosphodiester linkages: that is probably why Nature has selected the comparatively stable DNA for the storage of genetic information, whereas the more reactive mRNA is well suited for temporary information transport.

In the present work, it was found that inclusion of AMP and dAMP (as the respective disodium salts) within a MO-based *Ia3d* cubic phase had some unexpected consequences: (i) both AMP and dAMP were hydrolyzed at rates that were found to be exceptionally high when compared to those observed under similar conditions of pH, temperature, and concentration in aqueous solutions; (ii) hydrolysis reaction proceeded much faster for AMP- than for dAMP-containing samples; (iii) both nucleotides were effective in reducing the MO polar head area, thus inducing either the intercubic or the cubic to hexagonal phase transitions; (iv) the former is accelerated by the hydrogen phosphate dianion arising from AMP/dAMP hydrolysis under the described conditions; (v) the high concentration (6.0 wt %) of AMP and dAMP used in the second series of experiments induced an intercubic phase transition, even in freshly prepared samples; (vi) the *Pn3m* cubic phase obtained under these conditions did not present nucleotide hydrolysis rates comparable to those observed with the *Ia3d* cubic phase. Possibly, hydrolysis does not occur at all.

These findings trigger a number of considerations that could add information to the fascinating topic of phosphorylation/dephosphorylation control in biological contexts. The straightforward conclusion that can be drawn from the results outlined above is that the *Ia3d* cubic phase was specifically responsible for the observed hydrolysis. This deduction is corroborated by FT-IR and self-diffusion experiments that highlight the existence of specific interactions between the oxygen atoms of the phosphate moieties of the nucleotides and the hydroxyl groups of mono-olein.

The finding that specific interactions between phosphoesters and hydroxyl-containing molecules could take place, and in certain cases catalyze hydrolysis, is not new. Such a catalytic activity was definitely found for lanthanum hydroxide gels⁴³ (where the hydroxide character of the hydroxyl groups should be relatively low). Also ascorbic acid was found capable of promoting phosphoester hydrolysis (although in some cases it acts as a hydrolysis inhibitor!).⁴³

It is also worth noticing that the nucleotide phosphoryl was not transferred onto whatever nucleophile was present in our system (water, mono-olein, and (deoxy)ribose hydroxyl groups), but exclusively to water: no transphosphorylation products were found at all, but only (deoxy)adenosine and hydrogen phosphate dianion. The last observation, taken together with the others above, indicates that a hydroxyl group of mono-olein is involved in the phosphoester bond hydrolysis through a dissociative mechanism (possibly through a six-membered transition state): indeed, if the same hydroxyl group was involved in the formation of a phosphorane-like intermediate (thus following an associative mechanism), a phosphorylated mono-olein should be the main reaction product. As a point of fact, not even traces

of phosphoryl mono-olein could be found at the end of the observation time, but only remaining (d)AMP and HPO_4^{2-} .

But above all, the most interesting finding of the present study is the sharp difference in the hydrolysis rates of AMP and dAMP: to our knowledge, this is the first report of a substantial difference in the chemical behavior of the two nucleotides, exclusively based on the presence/absence of the 2'-hydroxyl group.

What could be the role of the 2'-OH in substantially enhancing the hydrolysis of AMP with respect to dAMP? On the nucleotides side, it should be envisaged how their inclusion in the *Ia3d* cubic phase could force or at least favor one (or more?) conformation, prone to closely interact with the MO-water interface to form the hypothesized key six-membered cyclic transition state. The possible conformations of the investigated nucleotide couple could be *syn* or *anti* with regard to the respective positions of the adenine base and the (deoxy)sugar, the former being more favored in solution whereas the latter may become important within the relatively narrow water channels of the studied phase. At any rate, the putative presence of the more compact *syn* conformation could well favor the close proximity between the phosphoryl moiety and the MO interface but should conceivably be void of any consequence in differentiating between the nucleotide couple AMP/dAMP. With concern to the (deoxy)ribose allowed conformations, the most common are C(3')-*endo* and C(2')-*endo*,⁴⁴ also keeping in mind that in dAMP the lack of the 2'-OH relieves some substituent crowding, and therefore the deoxyribose ring is presumably more flexible than the ribose is. On the other hand, in the C(3')-*endo* the 2'-OH would be somewhat less hindered than it would be in the alternative C(2')-*endo* conformation. Plainly, it is difficult to imagine that a *more flexible* molecule is *more hindered* with regard to its interaction with mono-olein hydroxyls. Rather, the absence of the 2'-hydroxyl group may account for a different positioning at the interface of the dAMP species, which renders less probable (but not impossible) the formation of the six-membered cyclic transition state that is believed to play a key role in the dissociative phosphoester hydrolysis.

Conclusions

Here, the hydrolysis of two nucleotides included within a cubic lipid matrix, namely AMP and its 2'-deoxy derivative dAMP, and the phase behavior provoked by their interaction with the lipid-water interface were thoroughly investigated.

As demonstrated by the FT-IR experiments, on the lipid side molecular recognition occurs essentially through the *sn-2* and the *sn-3* alcoholic OH groups of the MO polar head. Regarding the nucleotides, as indicated mainly by the ³¹P NMR self-diffusion measurements, the orthophosphate group is without any doubt involved in the recognition process. Nevertheless, at least to a certain extent, recognition must occur also via the sugar hydroxyl groups, as demonstrated by the dissimilar phase behavior reported for the inclusion of the two nucleotides. Clearly, the stronger or weaker adherence of the nucleotides to the interface caused by the different specific interactions comes into sight as the observed temperature-dependent phase behavior (at 1.5 wt %) and the different structural parameters (at 6 wt %) emphasized by SAXS.

The nucleotides-induced phase behavior can be visualized as follows. Anchorage of nucleotides to MO molecules at the

(43) Butcher, W. W.; Westheimer, F. H. *J. Am. Chem. Soc.* **1955**, *77*, 2420.

(44) Govil, G.; Saran, A. *J. Theor. Biol.* **1971**, *32*, 399.

lipid–water interface via hydrogen bonds reduces the thermal motions of the MO polar heads, thus causing a shrinking of the effective polar head areas. In turn, this phenomenon leads either to the intercubic *Ia3d* to *Pn3m* or to the cubic–hexagonal phase transitions. Upon hydrolysis reaction, the released hydrogen phosphate dianion accelerates the cubic–hexagonal phase transition.

Although far from the extraordinary rate enhancement caused by catalytic activity of enzymes, the nucleotides hydrolysis reaction observed here within the cubic lipid matrix occurs, according to a dissociative mechanism, several orders of magnitude faster than that in aqueous solution. As also suggested by the apparent activation energies, the mechanism underlying the hydrolysis reaction is the same for AMP and dAMP, though the reaction proceeds slower for the latter. This finding highlights a substantial difference in the chemical behavior of the two nucleotides which has never previously been observed. Remarkably, the hydrolysis mechanism appears to be highly specific

for the *Ia3d* phase. In fact, within the limits imposed by the experimental technique used, no hydrolysis was detected in the *Pn3m* phase.

On the whole, the results discussed here evidenced that the function of the lipid matrix constituting the water channel walls may not be just passively structural. Indeed, lipid molecules at the interface can also interact with defined substrates operating as a highly specific catalyst. Such a conclusion becomes particularly significant if the biological role of these bicontinuous cubic phases is taken into account.

Acknowledgment. Stefano Montaldo is kindly thanked for the IPMS representation. MIUR (PRIN 2008, grant number 2006030935) is acknowledge for financial support. The Scientific Park Polaris (Pula, CA, Italy) is acknowledged for free access to FT-IR and SAXD facilities.

JA1069745